



---

## Faculty Scholarship

---

2010

# Simultaneous Two-Dimensional Laser-Induced-Fluorescence Measurements Of Argon Ions

A. K. Hansen

Matthew Galante

Dustin McCarren

Stephanie Sears

E. E. Scime

Follow this and additional works at: [https://researchrepository.wvu.edu/faculty\\_publications](https://researchrepository.wvu.edu/faculty_publications)

---

### Digital Commons Citation

Hansen, A. K.; Galante, Matthew; McCarren, Dustin; Sears, Stephanie; and Scime, E. E., "Simultaneous Two-Dimensional Laser-Induced-Fluorescence Measurements Of Argon Ions" (2010). *Faculty Scholarship*. 674.

[https://researchrepository.wvu.edu/faculty\\_publications/674](https://researchrepository.wvu.edu/faculty_publications/674)

This Article is brought to you for free and open access by The Research Repository @ WVU. It has been accepted for inclusion in Faculty Scholarship by an authorized administrator of The Research Repository @ WVU. For more information, please contact [ian.harmon@mail.wvu.edu](mailto:ian.harmon@mail.wvu.edu).

# Simultaneous two-dimensional laser-induced-fluorescence measurements of argon ions<sup>a)</sup>

A. K. Hansen,<sup>b)</sup> Matthew Galante, Dustin McCarren, Stephanie Sears, and E. E. Scime  
*Department of Physics, West Virginia University, P.O. Box 6315, Morgantown, West Virginia 26506-6315, USA*

(Presented 18 May 2010; received 14 May 2010; accepted 28 May 2010;  
 published online 1 October 2010)

Recent laser upgrades on the Hot Helicon Experiment at West Virginia University have enabled multiplexed simultaneous measurements of the ion velocity distribution function at a single location, expanding our capabilities in laser-induced fluorescence diagnostics. The laser output is split into two beams, each modulated with an optical chopper and injected perpendicular and parallel to the magnetic field. Light from the crossing point of the beams is transported to a narrow-band photomultiplier tube filtered at the fluorescence wavelength and monitored by two lock-in amplifiers, each referenced to one of the two chopper frequencies. © 2010 American Institute of Physics. [doi:10.1063/1.3460630]

## I. INTRODUCTION

Laser-induced fluorescence (LIF) in plasmas provides nonperturbative, spatially resolved measurements of particle (ion or atom) velocity distribution functions.<sup>1</sup> LIF has been used in many types of plasma discharges, including helicon plasma sources, to measure ion flow, ion temperature, magnetic field strength, and plasma density.<sup>2–8</sup> Typically, these measurements are made at a single location in a plasma. By changing the direction of the injected beam, without necessarily changing the location of the detector, it is possible to measure the velocity distribution function for two velocity components.<sup>9,10</sup> Some research groups have performed planar LIF measurements in which a laser beam is spread into a sheet and used to illuminate a cross section of a plasma.<sup>11,12</sup> The induced fluorescence is then imaged with a camera, and a two-dimensional image of LIF intensity and flow along the direction of the laser beam was obtained. If the laser has a narrow enough linewidth, such diagnostic approaches can even provide spatially resolved measurements of ion temperature<sup>11</sup> without perturbing the plasma. Measurements of two ion velocity components using multiplexed LIF at a single location have been previously reported in thruster experiments.<sup>13–15</sup> In this work, we present the initial development of a multiplexed scheme on the Hot Helicon Experiment (HELIX) at West Virginia University,<sup>8</sup> made possible by recent upgrades to the LIF system, which allows simultaneous measurements of the ion velocity distribution function (IVDF) parallel and perpendicular to the magnetic field.

## II. THE HELIX DEVICE

The HELIX consists of a vacuum chamber, which is a 61 cm long Pyrex tube, 10 cm in diameter, connected to a 91 cm long stainless-steel chamber, 15 cm in diameter (Fig. 1). The stainless-steel chamber has one set of four 6 in.

Conflat<sup>™</sup> crossing ports in the center of the chamber and three sets of four 2 $\frac{3}{4}$  in. Conflat<sup>™</sup> crossing ports on either side, which are used for LIF diagnostic access. The locations of the ports used for this work are noted in Fig. 1. The opposite end of the stainless-steel chamber opens into a 2 m diameter space chamber, the Large Experiment on Instabilities and Anisotropies (LEIA).<sup>16</sup>

Ten electromagnets produce a steady-state axial magnetic field of 0–1400 G in the source; 800 G was used in the measurements reported here. The source gas is argon at neutral pressures of 1–10 mT, regulated by a precision mass flow controller; the pressure in these experiments was around 3 mT. During operation, the neutral pressure in LEIA ranges from four to ten times lower than the pressure in the plasma source. rf power of up to 2.0 kW over a frequency range of 6–18 MHz coupled into a 19 cm, half-wave, helix antenna is used to generate the steady-state plasma; 500 W at 9.5 MHz was used in the measurements reported here. The antenna is right-handed relative to the magnetic field direction and is designed to launch the  $m=+1$  helicon wave toward LEIA. A common electrical ground is used for the vacuum chambers and the rf amplifier. For the measurements reported here, the magnetic field in LEIA was zero.

## III. THE HELIX LIF SYSTEM

In a typical LIF measurement, the frequency of a very narrow bandwidth laser is swept across a collection of ions or atoms that have a thermally broadened velocity distribution. An atom or ion absorbs a photon when it is at the appropriate frequency in its rest frame. After a short time, depending on the lifetime of the excited state, the atom or ion emits a photon, either at the same or another frequency. Measuring the intensity of the emitted photons as a function of laser frequency constitutes a LIF measurement.

Our LIF laser system consists of a 10 W Spectra-Physics Millennium Pro diode laser that pumps a Sirah Matisse-DR tunable ring dye laser running rhodamine-6G dye. The dye laser is tuned to 611.6616 nm (vacuum wavelength) to pump the Ar-II  $3d^2G_{9/2}$  metastable state to the  $4p^2F_{7/2}$  state, which

<sup>a)</sup> Contributed paper, published as part of the Proceedings of the 18th Topical Conference on High-Temperature Plasma Diagnostics, Wildwood, New Jersey, May 2010.

<sup>b)</sup> Electronic mail: alex.hansen@mail.wvu.edu.

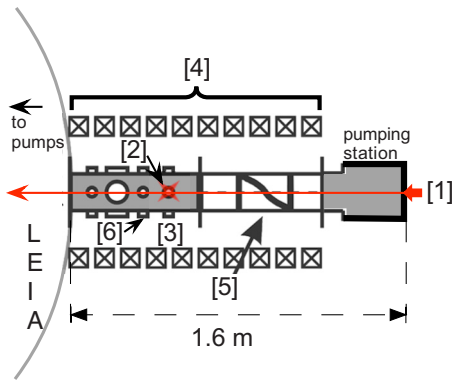


FIG. 1. (Color online) Schematic of the HELIX device, top view (Ref. 1). Parallel injection optics (Ref. 2), perpendicular injection optics (Ref. 3), collection optics, coupled to PMT (Ref. 4), magnets (Ref. 5), RF antenna (Ref. 6), and gas injection port.

then decays to the  $4s^2D_{5/2}$  state by emitting 461.086 nm (vacuum) photons. Approximately 5% of the output of the Matisse-DR is picked off via a beamsplitter for diagnostic purposes. The diagnostic beam is passed through an iodine cell for a consistent zero-velocity reference measurement. Fluorescent emission from the iodine cell is detected with a photodiode for each scan of the dye laser wavelength. The wavelength is also measured via a Bristol Instruments 621-VIS wavelength meter.

The remainder of the output is split with a 50-50 beam-splitter into two daughter beams, each of which is modulated by a Stanford Research Systems SR540 mechanical chopper. The two choppers run at different frequencies. Each daughter beam is coupled into a multimode, non-polarization-preserving optical fiber to transport laser light to the injection optics. One fiber connects to the parallel injection optics, and the other connects to the perpendicular injection optics (Figs. 1 and 2). The parallel injection optics consist of a 2.54 cm o.d. collimating lens, followed by an Oriel polarizer plus  $\frac{1}{4}$ -wave plate to circularly polarize the light exiting the fiber. With laser light of a single circular polarization injected

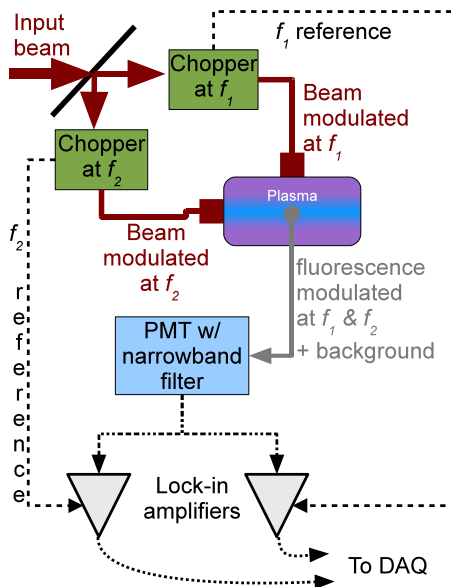


FIG. 2. (Color online) Cartoon of the HELIX LIF system.

along the source axis, only one of the two  $\sigma$  transitions, specifically the  $\Delta m = +1$  transition, is pumped. For absolute flow measurements, it is necessary to account for Zeeman splitting during analysis of the parallel injection data. The perpendicular injection optics consist of another 2.54 cm o.d. collimating lens and a linear polarizer, which is aligned with the magnetic field. The polarizer limits pumping to the  $\pi$  transitions ( $\Delta m = 0$ ); the much larger Zeeman splitting of the  $\sigma$  transition ( $\Delta m = \pm 1$ ) lines is avoided, and the IVDF is fit with a single thermally broadened Gaussian function. The internal Zeeman splitting of the  $\pi$  lines, Stark broadening, the natural linewidth of the absorption line, and the laser linewidth are ignorable in comparison. The two injection beams intersect at a single spatial location.

The collection optics consists of a multimode fiber cable coupled to a 2.54 cm outer diameter (o.d.) collimating lens with a matching numerical aperture (NA=0.22) to maximize light collection. The line of sight is perpendicular to both injection beams, and the lens is focused on their crossing point. The output of the fiber is filtered via a narrowband filter (1 nm bandwidth around 461 nm) and coupled into a narrowband, high-gain Hamamatsu photomultiplier tube (PMT). The PMT signal is composed of fluorescence radiation from the two injection beams, as well as background contributions from electron-impact-induced radiation and electronic noise. To eliminate the background contributions, the output of the PMT is teed into a pair of Stanford Research Systems SR830 lock-in amplifiers. Each lock-in is referenced to the mechanical chopper on each injection beam. The background, which is not correlated with either modulation frequency, is eliminated, and the fluorescence from the parallel and perpendicular injections is separated.

#### IV. OBSERVATIONS

In Fig. 3(a) is plotted the output of the iodine cell as a function of the shift in laser frequency from its central value as measured by the wavemeter. The central feature corresponds to the spectral line at  $16\,348.9427\text{ cm}^{-1}$ . In Fig. 3(b) are plotted the parallel (solid curve) and perpendicular (dashed curve) LIF signals. 8192 points are taken per scan, and thus for the 15 GHz window used for these data, this corresponds to 1.83 MHz per point. The difference in amplitudes between the parallel and perpendicular signals is because the gain from the perpendicular signal was amplified to compensate for weaker transmission in the perpendicular injection fiber. The perpendicular LIF signal has a similar signal-to-noise ratio to the parallel LIF signal.

To convert the LIF signals to IVDFs, the frequency axes are first shifted by using reference lines in the iodine reference cell signal to determine where the zero for frequency (or velocity) for the LIF transition should occur. A correction is then applied to remove the effect of Zeeman splitting from the frequency axis of the parallel LIF signal. Then the frequency axes are converted to velocities. In Fig. 4 are plotted the parallel (solid curve) and perpendicular (dashed curve) LIF signals as a function of velocity, i.e., IVDFs. The flow velocity and temperature are determined by fitting the IVDFs to Gaussians: the dotted curve for the parallel IVDF and the

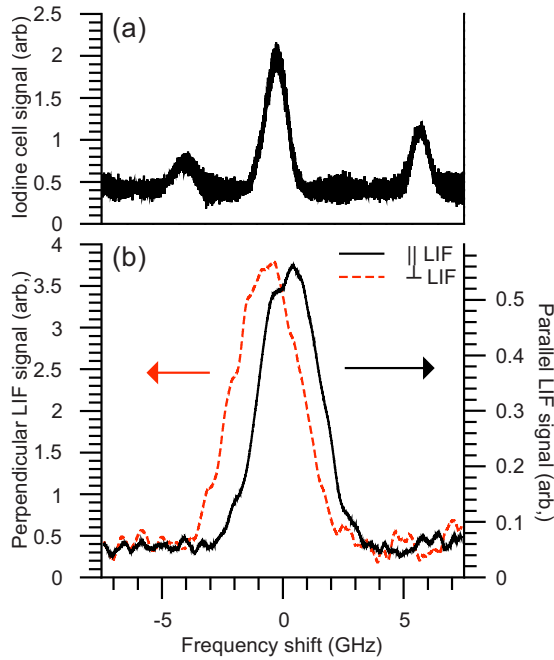


FIG. 3. (Color online) (a) Fluorescence signal from the iodine reference cell and (b) parallel (solid curve) and perpendicular (dashed curve) raw LIF signals, averaged over five scans.

dashed-dotted curve for the perpendicular IVDF. From these fits, the parallel flow is 270 m/s, the parallel temperature is 0.22 eV, the perpendicular flow is 370 m/s, and the perpendicular temperature is 0.27 eV. The finite perpendicular flow is probably azimuthal flow due to a slight misalignment of

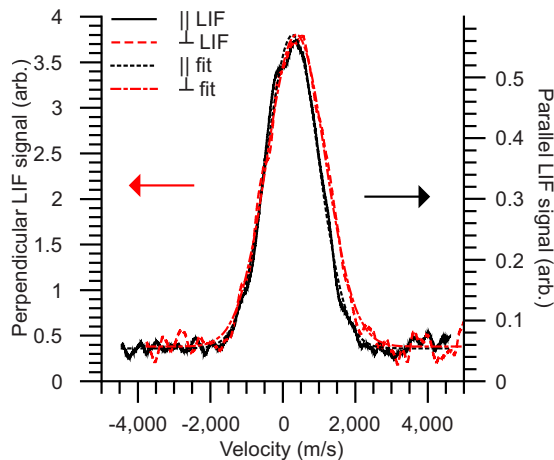


FIG. 4. (Color online) Parallel (solid curve) and perpendicular (dashed curve) IVDFs, averaged over five scans, along with Gaussian fits: dotted curve for parallel and dashed-dotted curve for perpendicular.

the overlap of the injection and collection volumes, i.e., the measurement was not performed exactly at  $r=0$  cm (cf. Ref. 10).

## V. DISCUSSION AND FUTURE PLANS

Our scheme is quite similar to that in Ref. 13; both involve simultaneous measurements using multiplexed LIF. There are some differences in detail: in Ref. 13, the zero-velocity reference is established using an optogalvanic cell, and the two injection beams are oblique rather than orthogonal. A more significant distinction is that the system in Ref. 13 was capable of measurements at only a single point in space and without temporal information; this diagnostic system is easily extended to utilize our capacity to measure the three-dimensional IVDF via simultaneous repositioning of the injection and collection optics,<sup>10</sup> as well as to perform time-resolved LIF measurements.<sup>17,18</sup> The capability of being able to perform time-resolved IVDFs in two dimensions simultaneously will allow us to investigate the full ion response to waves excited in the plasma. This technique is also easily extended to multiple detection locations as well as three (or more) injection beams.

## ACKNOWLEDGMENTS

This work was supported by NSF under Award No. PHY-0918526.

- <sup>1</sup>R. A. Stern and J. A. Johnson, *Phys. Rev. Lett.* **34**, 1548 (1975).
- <sup>2</sup>R. A. Stern, D. N. Hill, and N. Rynn, *Phys. Lett. A* **93**, 127 (1983).
- <sup>3</sup>D. N. Hill, S. Fornaca, and M. G. Wickham, *Rev. Sci. Instrum.* **54**, 309 (1983).
- <sup>4</sup>R. McWilliams and D. Sheehan, *Phys. Rev. Lett.* **56**, 2485 (1986).
- <sup>5</sup>J. M. McChesney, R. A. Stern, and P. M. Bellan, *Phys. Rev. Lett.* **59**, 1436 (1987).
- <sup>6</sup>D. A. Edrich, R. McWilliams, and N. S. Wolf, *Rev. Sci. Instrum.* **67**, 2812 (1996).
- <sup>7</sup>G. D. Severn, D. A. Edrich, and R. McWilliams, *Rev. Sci. Instrum.* **69**, 10 (1998).
- <sup>8</sup>E. E. Scime, P. A. Keiter, M. W. Zintl, M. M. Balkey, J. L. Kline, and M. E. Koepke, *Plasma Sources Sci. Technol.* **7**, 186 (1998).
- <sup>9</sup>W. A. Hargus, Jr. and M. A. Cappelli, *Appl. Phys. B: Lasers Opt.* **72**, 961 (2001).
- <sup>10</sup>R. Hardin, X. Sun, and E. E. Scime, *Rev. Sci. Instrum.* **75**, 4103 (2004).
- <sup>11</sup>A. D. Bailey, R. A. Stern, and P. M. Bellan, *Phys. Rev. Lett.* **71**, 3123 (1993).
- <sup>12</sup>F. M. Levinton and F. Trintchouk, *Rev. Sci. Instrum.* **72**, 898 (2001).
- <sup>13</sup>W. M. Ruyten and D. Keefer, *AIAA J.* **31**, 2083 (1993).
- <sup>14</sup>J. G. Liebeskind, R. K. Hanson, and M. A. Cappelli, *Appl. Opt.* **32**, 6117 (1993).
- <sup>15</sup>G. J. Williams Jr., T. B. Smith, F. S. Gulczynski III, B. E. Beal, A. D. Gallimore, and R. P. Drake, *AIAA Paper No. 99-2424* (1999).
- <sup>16</sup>E. E. Scime, P. A. Keiter, M. M. Balkey, R. F. Boivin, J. L. Kline, M. Blackburn, and S. P. Gary, *Phys. Plasmas* **7**, 2157 (2000).
- <sup>17</sup>I. Biloiu and E. Scime, *IEEE Trans. Plasma Sci.* **36**, 1376 (2008).
- <sup>18</sup>E. E. Scime, I. A. Biloiu, J. J. Carr, S. C. Thakur, M. Galante, A. Hansen, S. Houshmandyar, A. M. Keesee, D. McCarran, S. Sears, C. Biloiu, and X. Sun, *Phys. Plasmas* **17**, 055701 (2010).